Structural Studies of Myosin:Nucleotide Complexes: A Revised Model for the Molecular Basis of Muscle Contraction

Andrew J. Fisher,* Clyde A. Smith,* James Thoden,* Robert Smith,* Kazuo Sutoh,‡ Hazel M. Holden,* and Ivan Rayment*

*Department of Biochemistry and Institute for Enzyme Research, University of Wisconsin, Madison, Wisconsin 53705 USA, and ‡Department of Pure and Applied Sciences, University of Tokyo, Komba, Tokyo 153, Japan

ABSTRACT The structures of the MgADP-beryllium fluoride and MgADP-aluminum fluoride complexes of the truncated myosin head from *Dictyostelium* myosin II are reported. These reveal the location of the nucleotide complex and define the amino acid residues that form the active site. The tertiary structure of the beryllium fluoride complex is essentially identical to that seen previously in the three-dimensional structure of chicken skeletal muscle myosin. By contrast, significant domain movements are observed in the aluminum fluoride complex. These structural findings form the basis of a revised model for the structural basis of the contractile cycle. It is now suggested that the narrow cleft that splits the central 50-kDa segment of the heavy chain provides not only the communication route between the nucleotide-binding pocket and actin but also transmits the conformational change necessary for movement.

INTRODUCTION

Previous x-ray crystallographic studies of skeletal muscle myosin subfragment-1 have established the overall domain structure and tertiary fold of this complex molecular aggregate (Rayment et al., 1993b). From the preliminary efforts to dock myosin onto actin, it was suggested that actomyosin-based motility arises through a series of domain movements prompted by the binding of nucleotide to myosin followed by rebinding to actin (Rayment et al., 1993a). Although this work resolved many issues concerning the architecture of the molecule, it posed many more questions concerning the molecular details of how this protein functions as a molecular motor. The most fundamental question left unanswered by the structural hypothesis was: what is the exact nature of the conformational changes that underlie the conversion of chemical energy into directed movement?

The three-dimensional structure of chicken skeletal myosin subfragment-1 is characterized by a series of clefts and pockets that divide the protein into distinct domains (Rayment et al., 1993b). The most prominent cleft splits the 50-kDa segment of the heavy chain into two distinct domains and extends from the base of the nucleotide-binding pocket to the actin-binding face. This observation, coupled with the preliminary attempt to dock myosin onto actin within the constraints of the image reconstruction, suggested that domain movements associated with this cleft play a major role in the energy transduction process. It was proposed that closure of the cleft occurs when myosin binds tightly to actin and that this state is mutually exclusive with the binding of ATP. In a complementary manner, it was hypothesized that when ATP binds, it opens the cleft and reduces the affinity of myosin for actin. Thereafter, it was suggested that the nucleotide-binding pocket closes around the base to generate a "conformationally bent" state that is primed to generate movement of the thick filament relative to actin when myosin rebinds to actin. In the original work, it was indicated that the nature of the conformational changes were likely to be too large to be modeled correctly without additional experimental information. To overcome this problem, the three-dimensional structure of a truncated myosin head from *Dictyostelium discoideum* myosin II (S1Dc) has been determined in the presence of MgADP and beryllium fluoride. A related structure of S1Dc complexed with MgADP and aluminum fluoride has also been determined.[1]

MATERIALS AND METHODS

The myosin head was truncated at the start of the light chain-binding region to yield a globular molecule, of molecular mass ~87 kDa, that still retains the ATPase activity and limited ability to support movement (Itakura et al., 1993). S1Dc was prepared as described before (Itakura et al., 1993), with the exception that an ATP affinity column was used as the final column step in place of hydroxyapatite (provided by Ralph Yount, Washington State University, Pullman, WA). Crystals of the beryllium fluoride MgADP S1Dc complex (MgADP · BeFx · S1Dc) were grown by microbatch from 8.5% polyethyleneglycol 8000, 25 mM HEPES, pH 7.0, 1.5% methanepentanediol, 170 mM NaCl, 1.8 mM ADP, 1.8 mM $MgCl_2$, 1.8 mM $BeCl_2$, 9 mM NaF, and 3 mM DTT at 4°C with a protein concentration of ~4 mg/ml. The crystals of the aluminum flouride complex (MgADP · AlF_4 · S1Dc)[2] were grown under similar conditions except that the beryllium chloride was replaced by $Al(NO_3)_3$. The protein was not chemically modified.

Address reprint requests to Dr. Ivan Rayment, Institute for Enzyme Research, University of Wisconsin, 1710 University Avenue, Madison WI 53705. Tel.: 608-262-0437; Fax: 608-265-2904.

0006-3495/95/04/19s/10 $2.00

[1] In the initial abstract prepared for the Biophysical Discussions, it was reported that the structure of S1Dc was also determined in the absence of nucleotide. However, as noted at that time, the active-site pocket was not entirely empty. It now appears that those crystals were of a complex of S1Dc and magnesium pyrophosphate. This structure was not discussed or presented in detail during the discussions and will be published elsewhere (Smith et al., 1995).

[2] The exact composition of the beryllium fluoride species in the complex is unknown, whereas the aluminum fluoride complex is believed to contain $(AlF_4)^-$ (Henry et al., 1993; Maruta et al., 1993). Consequently, these metallofluoride complexes will be designated as BeF_x and AlF_4.

Crystals of MgADP · BeFx · S1Dc belong to space group $P2_12_12$ with unit cell parameters of $a = 105.3$ Å, $b = 182.6$, and $c = 54.7$ Å and contain one molecule per asymmetric unit. These crystals diffract to 1.8 Å resolution with synchrotron radiation; however, in this study data to 2.0 Å resolution were used. An initial x-ray data set was recorded to 2.6 Å resolution on a Siemens HI-STAR double-detector system at 4°C (R_{merge} 11.0%, 98% complete) and extended to higher resolution at the Stanford Synchrotron facility (SSRL) with an MAR image plate detector (R_{merge} 3.7%, 82% complete). In contrast, crystals of MgADP · AlF_4 · S1Dc belong to the orthorhombic space group, $C222_1$, with unit cell dimensions of $a = 87.9$ Å, $b = 149.0$ Å, and $c = 153.8$ Å and contain one molecule per asymmetric unit. X-ray data were collected from a single crystal at −160°C on a Siemens HI-STAR Area Detector (R_{merge} 6.1%, 96% complete).

The structures of both complexes were solved by molecular replacement (Rossmann, 1972) and refined with a combination of molecular dynamics and conventional restrained least-squares with the programs X-PLOR and TNT (Brünger, 1990; Tronrud et al., 1987). The structure of MgADP · BeFx · S1Dc was determined first from a model derived from the structure of chicken skeletal myosin subfragment 1. The experimental details will be described elsewhere (A. J. Fisher et al., unpublished data). The final model for MgADP · BeFx · S1Dc includes a total of 743 residues, 375 water molecules, and the nucleotide complex. The final R factor between the observed and calculated data was 19.1% for all data recorded between 30 and 2.0 Å resolution where the root-mean-square (rms) deviation from ideality for the bond lengths, angles, and trigonal planes was 0.015 Å, 2.26°, and 0.007 Å, respectively. A section of representative electron density of the protein is shown in Fig. 1.

The aluminum fluoride complex was solved by Molecular Replacement (Rossmann, 1972) from the refined MgADP · BeFx · S1Dc structure. A total of 646 residues were included in the present model together with 104 water molecules and the nucleotide complex. Most of the residues between Asn-2 and Lys-690 are well defined. However, the COOH-terminal 70 residues appear to adopt multiple conformations in the crystal and have not been modeled at present. The current R factor between the observed and calculated data is 24.2% for all data between 30 and 2.6 Å resolution, where the rms deviation from ideality for the bond lengths, angles, and planes was 0.013 Å, 2.39°, and 0.016 Å, respectively. The coordinates for both structures have been deposited in the Brookhaven Protein Data Bank.

RESULTS

MgADP · BeF_x · S1Dc

The structure of MgADP · BeFx · S1Dc will be described first because this model is more complete and because it is more similar to that of chicken skeletal myosin subfragment 1. The overall topology of the protein will be described with respect to the three major tryptic fragments of skeletal muscle myosin S1, the NH_2-terminal 25-kDa, central 50-kDa, and COOH-terminal 20-kDa fragment (Balint et al., 1975; Mornet et al., 1979; Cooke, 1986). Fig. 2 *a* shows a stereo representation of MgADP · BeFx · S1Dc oriented such that the cleft that splits the 50-kDa segment of the heavy chain is clearly visible. Fig. 2 *b* shows the corresponding fragment of chicken skeletal myosin subfragment 1 in the same orientation. It is immediately obvious that the domain structures of these two molecular fragments are remarkably similar. Indeed, the rms difference between 569 equivalent α-carbons in chicken and *Dictyostelium* myosin is 1.3 Å. This is only slightly larger than the expected difference of 1.1 Å for proteins that share the same function and exhibit 47% identity (Chothia and Lesk, 1986).The protruding β-barrel of the NH_2-terminal segment of MgADP · BeFx · S1Dc has the same topology as that observed in chicken skeletal S1 even though the sequence identity is only 36% (Warrick and Spudich, 1987). This part of the molecule was excluded from the phasing model in the structure determination and was built independently; thus, it serves to confirm the chain tracing for both proteins. It is noteworthy that the narrow cleft that splits the 50-kDa segment of the heavy chain is equally open in both chicken and *Dictyostelium* structures, and that there is surprisingly little change in the conformation of the nucleotide-binding pocket.

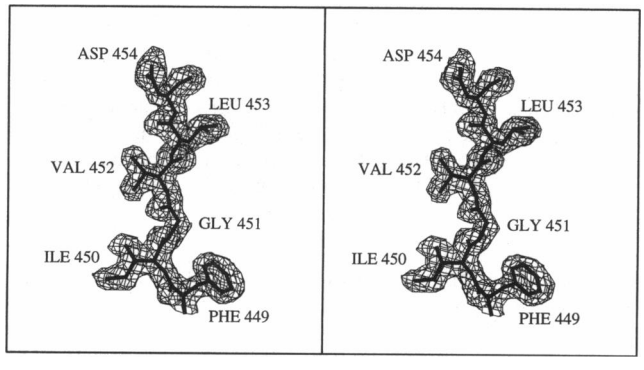

FIGURE 1 Representative electron density for a segment of the MgADP · BeF_x · S1Dc structure close to the crossover between the upper and lower domains of the 50-kDa segment. The majority of the electron density in the central segment of the myosin heavy chain is of this quality in the MgADP · BeF_x · S1Dc complex. Fig. 1 was prepared from a plot file generated from the molecular graphics program FRODO (Jones, 1985) and drawn with the program MOLVIEW (Smith, 1993).

Nucleotide-binding pocket in MgADP · BeF_x · S1Dc

The structure of MgADP · BeFx · S1Dc contains unambiguous electron density for an Mg^{2+} ion, ADP, and a beryllium trioxyfluoride. The nucleotide resides in the pocket formed by the interface of the NH_2-terminal and central 50-kDa segments of the heavy chain, as was suggested previously based on the location of the phosphate-binding loop and amino acid residues identified by photochemical labeling studies (Walker et al., 1982; Yount et al., 1992). The purine ring and ribose lie above the plane of the seven-stranded β-sheet that forms the major structural motif in the myosin head as shown in Fig. 2 and in more detail in Fig. 3. The purine ring lies against the 25-kDa segment of the heavy chain in the base of the pocket. It is enveloped by Arg-131, which is of interest because the equivalent tryptophan residue in skeletal muscle myosin has been implicated as part of the purine-binding site from photolabeling studies (Yount et al., 1992).

The α- and β-phosphate groups and the beryllium fluoride moiety make extensive stereospecific interactions with the protein, whereas the ribose and purine ring make proportionately far fewer. The overall geometry of the MgADP · BeF_x complex is consistent with the structure of an ATP analog, where a terminal oxygen of the β-phosphate forms a pseudo-bridging oxygen to the beryllium atom. This analog is sandwiched between the phosphate-binding loop on one

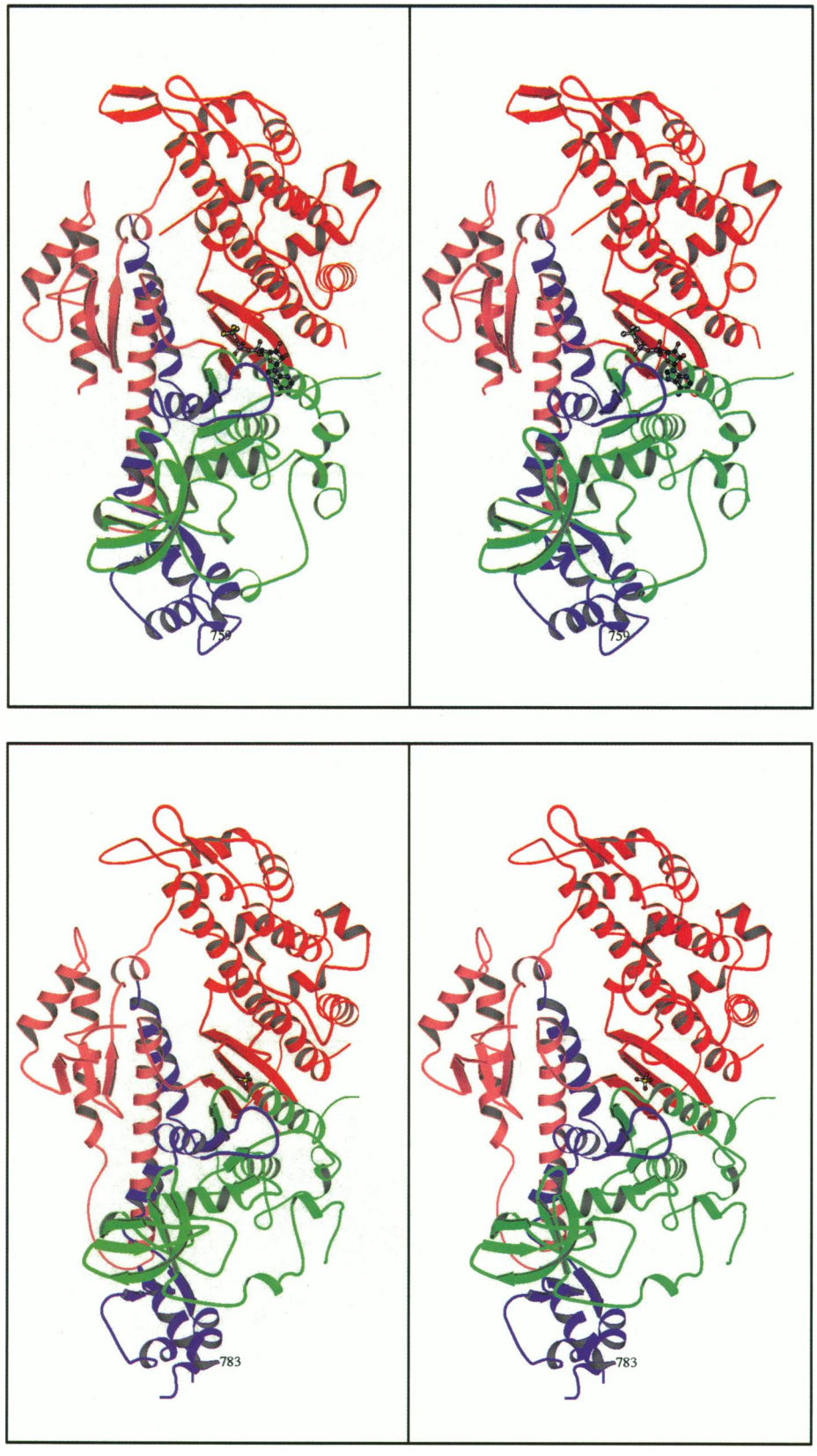

FIGURE 2 Stereo ribbon representation of (*A*) the MgADP · BeF_x · S1Dc complex of the truncated *Dictyostelium* myosin and (*B*) the corresponding fragment of chicken skeletal myosin subfragment-1. Both models are in the same orientation. The heavy chain is displayed in green, red/pink, and blue to delineate the NH_2-terminal, central (upper and lower domains), and COOH-terminal fragments that extend from residues Asn-2 to Ala-205, Gly-209 to Ala-621, and Phe-627 to Ala-759, respectively. These segments are separated by disordered loops in the x-ray structure that were identified previously in skeletal muscle myosin by mild tryptic cleavage of the myosin head, resulting in fragments of approximate molecular mass 25, 50, and 20 kDa, respectively (Balint et al., 1975; Mornet et al., 1979). The same nomenclature is retained for the respective segments in *Dictyostelium* myosin. The upper and lower domains of the central 50-kDa segment of the heavy chain are displayed in red and pink to differentiate between these components of the structure. Figs. 2–6 were prepared with the molecular graphics program MOLSCRIPT (Kraulis, 1991).

side and a loop from the central 50-kDa segment (Asn-233 to Gly-240) on the other. The beryllium fluoride moiety protrudes downwards into the small pocket that lies at the apex of the cleft that separates the upper and lower domains of the 50-kDa segment of the heavy chain (Fig. 3). The region around the metallofluoride moiety will be referred to as the γ-phosphate pocket. Details of the hydrogen-bonding pattern will be published elsewhere (A. J. Fisher et al., unpublished data).

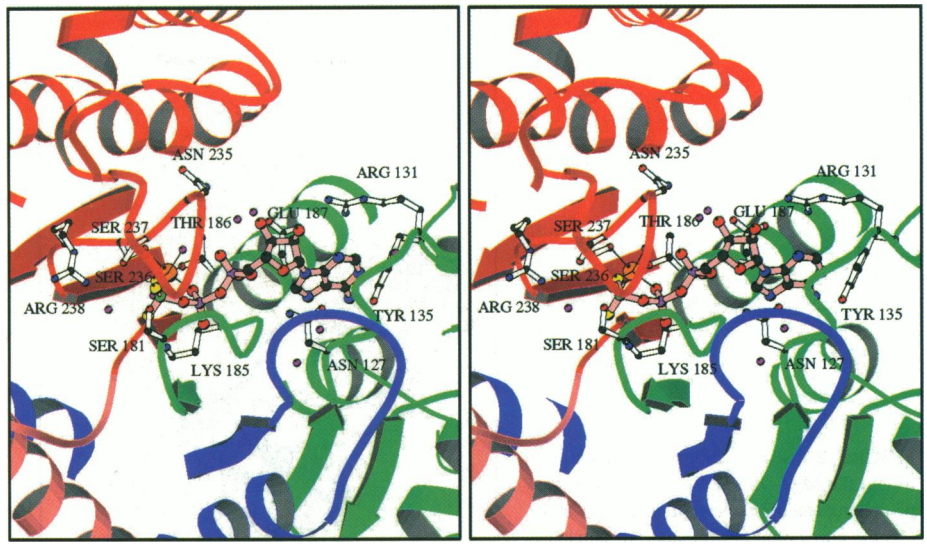

FIGURE 3 Stereo ribbon representation of the nucleotide binding region of the MgADP · BeF_x · S1Dc complex, viewed parallel to the seven-stranded β-sheet that forms the major tertiary structural element in the myosin motor domain. The myosin heavy chain is depicted with the same color scheme as in Fig. 2. This orientation shows the location of the nucleotide and its associated magnesium ion. The phosphate-binding site is located in the middle of the large β-sheet that forms the major structural motif in the myosin head and lies at the COOH-terminal end of the central β-strand. In this figure the MgADP · BeF_x is drawn with pink bonds, beryllium in green, carbon in black, fluorine in yellow, Mg^{2+} in orange, nitrogen in blue, oxygen in red, H_2O in magenta, and side chains that interact with the nucleotide with white bonds.

MgADP · AlF_4 · S1Dc

The structure of the aluminum fluoride nucleotide complex reveals a significant difference between the orientation of the upper and lower domains of the central 50-kDa segment of the myosin heavy chain relative to that seen in MgADP · BeFx · S1Dc. Fig. 4 reveals that the cleft separating these two domains has closed partially and that this movement displaces the region associated with the reactive cysteines in skeletal muscle. This difference arises as a consequence of the differences in the metallofluoride moiety in the γ-phosphate pocket.

The coordination of MgADP in the aluminum fluoride complex with S1Dc is essentially identical to that observed in MgADP · BeFx · S1Dc. In addition, unambiguous electron density is visible for a planar $(AlF_4)^-$ moiety coordinated to one of the terminal oxygen atoms of the β-phosphate of ADP. These form a square pyramidal arrangement of ligands around the aluminum atom. Density for an additional water molecule, which is expected to complete the anticipated octahedral coordination sphere of the aluminum atom, is ill defined and has not been included in the present model. The overall geometry of the aluminum and its associated ligands is very similar to that observed recently in the structures of the G protein $G_{i\alpha 1}$ and transducin α-complex with GDP and aluminum fluoride (Coleman et al., 1994; Sondek et al., 1994).

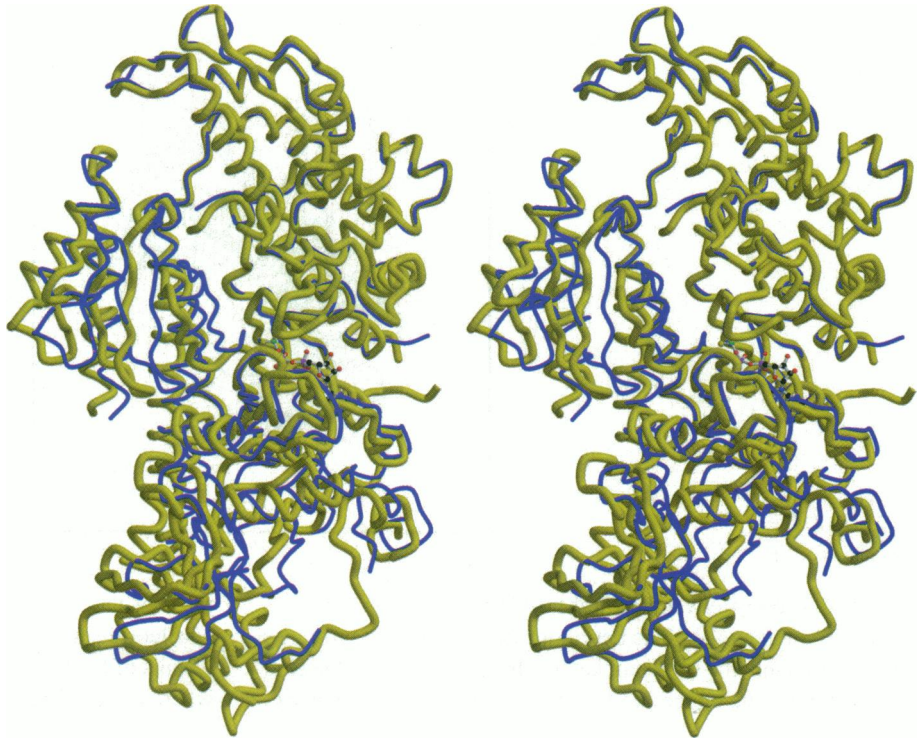

FIGURE 4 Stereo comparison of MgADP · BeF_x · S1Dc and MgADP · AlF_4 · S1Dc. The beryllium fluoride complex is depicted as a thicker coil. In those locations that the two models are identical, only the MgADP · BeF_x ·S1Dc structure is visible. The figure was prepared with MOLSCRIPT and Raster 3D (Merrit and Murphy, 1994).

The Al—O bond distance to the β-phosphate is longer than the corresponding distance observed in the beryllium fluoride complex (2.0 vs. 1.57 Å, respectively). This suggests that the aluminum fluoride complex is an analog of the transition state for hydrolysis of ATP rather than either the pre-hydrolysis (ATP) or post-hydrolysis (ADP, P_i) states. The structures of the GDP, $(AlF_4)^-$ complex in G protein $G_{i\alpha 1}$ and transducin-α (Coleman et al., 1994; Sondek et al., 1994) have been interpreted similarly.

The displacement of the aluminum atom, relative to the location of beryllium, and the longer Al—F bond distance compared with Be—F (1.8 compared with 1.55 Å, respectively) allows one of the fluorine ligands to form a short hydrogen bond to the amide hydrogen of Gly-457. The corresponding interaction is not possible in the beryllium fluoride complex because this moiety is much more compact. Formation of this new hydrogen bond is accomplished via changes in the main chain conformational angles for two residues, Ile-455 and Gly-457. Both of these residues are completely conserved in the myosin superfamily (Warrick and Spudich, 1987). Four additional hydrogen bonds and salt links are formed between the upper and lower domains of the 50-kDa segment that stabilize this rearrangement (Fisher et al., 1995). The overall consequence of these new interactions is a rotation of the lower domain by 5° relative to the upper domain. This generates a movement of approximately 5 Å in the position of residues at the outer edge of the cleft that splits the 50-kDa segment of the heavy chain.

Partial closure of the cleft prompts a rearrangement of the COOH-terminal segment of the heavy chain associated with the reactive sulphydryl groups in skeletal muscle. In particular, the helix that separates Cys-678 and Thr-689 (these residues are analogous to SH2 and SH1 in skeletal muscle myosin) is displaced by more than 2.5 Å and rotates by more than 10°. Unfortunately, the polypeptide chain beyond Thr-689 is not ordered in the crystal lattice in MgADP · AlF_4 · S1Dc. This most likely arises because of the conformational freedom introduced in the molecule due to the absence of the essential light chain. Even so, the observed rearrangement suggests that the shape of myosin S1 changes on hydrolysis of ATP.

One of the consequences of the partial closure of the cleft is reduced access of solvent to the γ-phosphate pocket. In a space-filling representation of the MgADP · BeFx · S1Dc complex (Fig. 5a), the beryllium fluoride moiety can be seen at the apex of the cleft from the outside of the molecule. This strongly suggests that the beryllium fluoride moiety, and by analogy ATP, is accessible to solvent when the molecule adopts this conformation. In contrast, the aluminum fluoride moiety is not visible from the solvent because of closure of the cleft (Fig. 5 *b*) and, thus, has reduced access of the γ-phosphate pocket to the solvent. If the structure observed in MgADP · AlF_4 · S1Dc complex mimics the transition state for hydrolysis, then the conformational change observed here may account for the formation of the metastable myosin:ADP,P_i state.

The space filling representations of the beryllium and aluminum fluoride complexes of S1Dc illustrate several other interesting features of the nucleotide-binding site. When the nucleotide-binding pocket is viewed from above the seven-stranded β-sheet (Fig. 5 *c*), it can be seen that the purine base is covered by Arg-131, whereas the 2′ and 3′ oxygen atoms of the ribose are exposed to solvent. This arrangement explains why a large variety of functional groups including spin-labels, fluorophores, and photolabels can be attached to the ribose ring in these positions without affecting function (Crowder and Cooke, 1987; Cremo et al., 1990; Cole and Yount, 1990). In addition, this orientation shows that the magnesium ion is partially visible, whereas the α- and β-phosphate groups and the beryllium fluoride moiety are

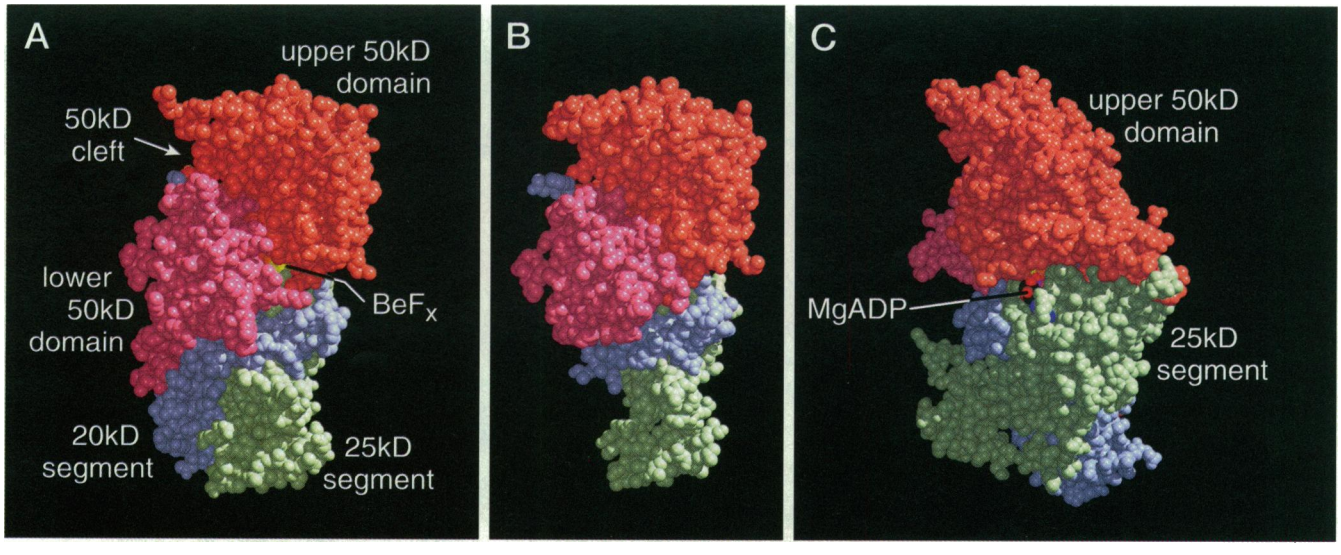

FIGURE 5 Space-filling representations of MgADP · BeF_x · S1Dc (*a*, *c*) and MgADP · AlF_4 · S1Dc (*c*). *a* and *b* are oriented to look into the cleft that splits the upper and lower domains of the 50-kDa segment of the heavy chain. *c* is oriented to view the nucleotide-binding pocket from above the seven-stranded β-sheet and reveals the extent to which the purine base and ribose are buried in the active site. The figure was prepared with MOLSCRIPT and Raster 3D (Merrit and Murphy, 1994).

almost completely buried. This suggests that the phosphate ion resulting from the hydrolysis of ATP cannot leave the active site via the same route that the nucleotide entered. These views of the molecule confirm the suggestion by Ralph Yount that myosin is a "back-door" door enzyme in which the hydrolysis products leave the active site by a different route from which they enter (Yount et al., 1995; Gilson et al., 1994).

DISCUSSION

The first conclusion from the structures of both MgADP · BeFx · S1Dc and MgADP · AlF_4 · S1Dc is that reductive methylation did not change the tertiary structure of the chicken skeletal muscle myosin in any major way; therefore, that structure remains a good model for the intact myosin head. This is in agreement with the control studies of the effect of reductive methylation on lysozyme and the kinetic studies of modified myosin (Rypniewski et al., 1993; White and Rayment, 1993). The second conclusion is that the nucleotide-binding pocket does not change significantly when nucleotide binds. This is consistent with the fluorescence quenching experiments of Cooke and co-workers (Franks-Skiba et al., 1994; Franks-Skiba and Cooke, 1995). Together this information suggests that the nucleotide-binding pocket, or at least that part associated with binding the purine ring, does not close or experience any major conformation changes during the contractile cycle.

Revised model for the contractile cycle

The initial model for the contractile cycle based on the x-ray structures of actin and myosin and the image reconstruction of the actomyosin complex suggested that the narrow cleft that splits the central 50-kDa segment of the heavy chain plays a central role in communicating between the nucleotide-binding pocket and the actin-binding interface. At that time, it was believed that the conformational change in the molecule that was responsible for the powerstroke arose from closure of the nucleotide binding pocket. The structures described above and the fluorescence-quenching experiments (Franks-Skiba et al., 1994; Franks-Skiba and Cooke, 1995) clearly indicate that the nucleotide-binding pocket (at least that part associated with ADP) does not change enormously in the contractile cycle. It is now suggested that the major conformational changes in the myosin head are associated with the domains that lie beneath the seven-stranded β-sheet and that these changes affect the status of the cleft that separates the upper and lower domains of the 50-kDa segment of the heavy chain.

The importance of the cleft that separates the upper and lower domains of the central 50-kDa segment of the heavy chain is highlighted by the presence of many highly conserved amino acid residues on the inner surfaces of this cleft (Fig. 6). In addition, a substantial number of residues that line the cleft are hydrophobic. It is unusual to observe any conserved residues exposed to solvent unless they fulfill an important structural or biochemical function. It is even more unusual to find exposed and conserved hydrophobic residues because this would be expected to be thermodynamically unstable. Examination of the upper and lower surfaces of the cleft suggests that these are complementary. Preliminary attempts to close the cleft, through changes in the main chain conformational angles around Gly-457, reveal that a rotation of approximately 10°, coupled with a movement of 10 Å of the lower domain away from the region associated with the reactive cysteine residues, is sufficient to close completely the cleft and achieve approximate complementarity between the two domains (data not shown). If such a movement does occur when myosin binds to actin, it is predicted that the effect will be transmitted from the lower domain to the COOH terminus of the myosin head via the 20-kDa region and through the essential and regulatory light chain. Initial attempts to propagate these movements

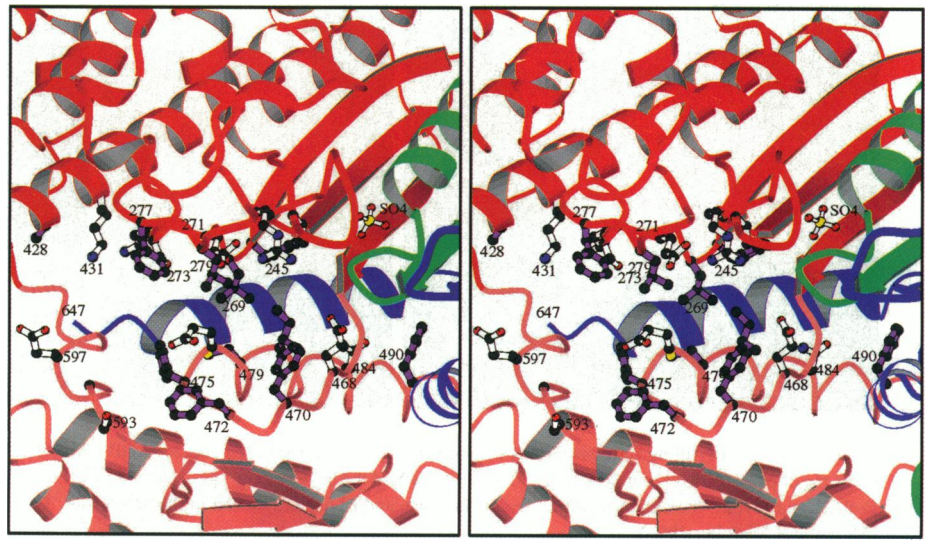

FIGURE 6 Stereo ribbon representation of the conserved and hydrophobic residues in chicken skeletal myosin S1 that extend into the cleft that splits the central 50-kDa segment of the heavy chain. The absolutely conserved residues on the upper face of the cleft include Thr-237, Arg-245, Gly-247, Tyr-268, Leu-269, Glu-271, Lys-272, Arg-273, Ala-428, and Lys-431. The lower face includes Glu-468, Glu-476, Ile-480, Asn-484, Leu-487, and Asn-597. There are several locations in the cleft where an exposed hydrophobic always resides; for example, Phe-470, Phe-475, Phe-490, Trp-593, and Leu-594 (Warrick and Spudich, 1987) (chicken skeletal muscle myosin sequence). The hydrophobic residues that line the cleft are displayed with purple bonds.

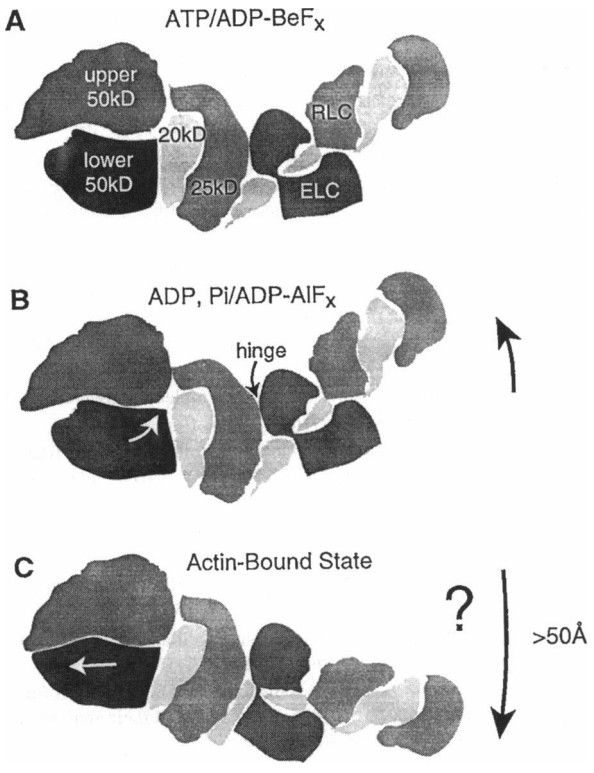

FIGURE 7 Schematic drawing of the conformational changes in the myosin head suggested to occur in the transition from S1:ATP through S1:ADP.P_i to the rigor complex (*a*, *b*, and *c*, respectively). In this model, the conformational changes are associated with movement of the lower domain of the central 50-kDa segment in response to ATP, ADP · P_i, and actin. For the purpose of illustration, the upper domain of the central 50-kDa segment is maintained in the same orientation throughout the figure. This is not an integral feature of the model, because the orientation of the upper and lower domains of the 50-kDa segment, at the above points in the contractile cycle, will depend on which component interacts with actin first.

through the myosin head, while conserving the domain-domain interfaces between the myosin heavy chain and essential light chain, indicate that a movement of the tail by ~40 Å can be accomplished easily. This modeling was carried out starting from the structure of chicken myosin S1 and did not include the conformational change in the COOH terminus predicted to occur at the transition state based on the structure of MgADP · AlF_4 · S1Dc. Combination of these two conformational changes would result in a substantially larger movement of the tail. A schematic representation of this structural change is shown in Fig. 7. This leads to a new model for the contractile cycle in which this cleft plays a greater role than previously suggested.

The revised hypothesis for the contractile cycle retains many of the features of the earlier model (Rayment et al., 1993a; Rayment and Holden, 1994). Starting from the rigor state,[3] the addition of ATP is suggested to open the cleft that splits the central 50-kDa region of the heavy chain and thoroughly disrupt the orientationally specific, strong actin-myosin interaction. This process is predicted to be a multistep process that initially allows the interaction to be broken without bending the molecule to a great extent, thus avoiding any reversal of the powerstroke. After the reduction of the affinity of myosin for actin, ATP is predicted to cause the molecule to bend partially relative to the actin-bound state (Fig. 6 *a*). The overall conformation of the myosin head in the ATP-bound state is predicted to be very similar to that observed in the structure of chicken skeletal myosin S1. It is conceivable that in the ATP-bound state, the myosin head is retained in close proximity to actin through a weaker ionic interaction provided by the loops on the myosin surface, such as that between the 50- and 20-kDa segments. This interaction is envisaged to be less stereospecific and provide extensive rotational freedom to the myosin head.

After or during hydrolysis of ATP, a further conformational change in the myosin head is predicted to occur. Based on the structure of MgADP · AlF_4 · S1Dc, this change is predicted to generate a molecule that is "fully primed" for the subsequent powerstroke (Fig. 7 *b*). This final conformational change is most likely the origin of the stability of the ADP,P_i state that serves to reduce the premature release of hydrolysis products.

Rebinding of myosin to actin is again predicted to be a multistep process involving several conformational states for myosin, in which the first stage is the formation of the weak ionic interaction followed by a stronger but stereospecific interaction with actin. In principle, the initial interaction between myosin and actin could be between either the upper or lower domains of the 50-kDa segment of the heavy chain. At this time, it is not clear which of these alternatives occurs. However the critical feature of the model is a requirement that the myosin head be in a specific orientation relative to actin before the onset of tight binding or the initiation of the powerstroke. Formation of a strong binding interaction between myosin and actin is suggested to cause the lower domain of the 50-kDa segment of the heavy chain to translate and rotate relative to the upper domain to allow release of the phosphate from the base of the nucleotide-binding pocket and close the cleft that separates these two domains (Fig. 7 *a*). As a consequence of this movement, the COOH-terminal 20-kDa segment of the heavy chain is predicted to cause the light chain-binding motif to rotate, thus generating a powerstroke. In the new model for the contractile cycle, a substantial fragment of the heavy chain would maintain the same orientation relative to actin throughout the powerstroke (defined as that part of the contractile cycle that the myosin head generates useful work). The conformational changes are predicted to occur in the COOH-terminal segment of the heavy chain.

Previously, it was suggested that the conformational change responsible for the powerstroke was centered on the nucleotide-binding pocket. This implied that the center of rotation for this movement must be close to the base of the nucleotide-binding pocket. The current hypothesis suggests

[3] It is presumed here that the structure observed in the rigor state represents the end of the power stroke.

that the conformational changes are induced by movement of the lower domain of the 50-kDa segment that are transmitted via the 20-kDa segment to the NH_2-terminal domain of the essential light chain and, hence, onto the rest of the head. To generate a rotational movement of the COOH terminus of the myosin head from these rearrangements, there must be a fulcrum or hinge present within the molecule. It is suggested that this hinge is represented by the interaction between the COOH-terminal domain on the essential light chain and the 25-kDa segment of the heavy chain associated with the edge of the nucleotide-binding pocket (Fig. 7 *b*). This expanded role for the essential light chain is consistent with the results from kinetic and in vitro motility studies of the function of this light chain reported by Lowey and co-workers at this meeting.

CONCLUSION

The most remarkable feature of the *Dictyostelium* truncated myosin head is its similarity in the presence of nucleotide to the structure of the chicken skeletal myosin S1. This suggests that the overall tertiary fold of the nucleotide-binding pocket associated with the ADP fraction of the nucleotide is very similar in solution and when it is bound to substrate. The current structural results emphasize the importance of the narrow cleft that splits the 50-kDa segment in the molecular origin of myosin based motility. They suggest further that it functions not only in sensing the presence of the γ-phosphate of ATP but is also responsible for transducing the conformational change that results in the powerstroke. The new information derived from the structure of the truncated *Dictyostelium* head shifts the location of the conformational change in the structural hypothesis from the nucleotide-binding pocket to the reactive sulfhydryl region of the molecule. However, it does not change the fundamental concept that domain movements underlie the molecular basis of muscle contraction.

We thank G. H. Reed and W. W. Cleland for helpful discussions.
This work was supported by National Institutes of Health grant AR35186 to I. Rayment. C. A. Smith is a Fogarty International Research Fellow TW05194. A. J. Fisher and J. Thoden are supported by National Service Research Award fellowships AR08304 and GM15950, respectively. K. Sutoh is supported by a grant-in-Aid from the Minister of Education, Science and Culture 06404081 and the Mitsubishi Foundation and the Ueha Memorial Foundation.

REFERENCES

Balint, M. 1975. The substructure of heavy meromyosin, the effect of Ca^{2+} and Mg^{2+} on the tryptic fragmentation of heavy meromyosin. *J. Biol. Chem.* 250:6168–6177.

Brünger, A. T. 1990. X-PLOR Version 3.1: A System for Crystallography and NMR. Yale University, New Haven, CT.

Chothia, C., and A. M. Lesk. 1986. The relationship between the divergence of sequence and structure in proteins. *EMBO J.* 5:823–826.

Cole, D., and R. G. Yount. 1990. *J. Biol. Chem.* 265:22547–22546.

Coleman, D. E. et al. 1994. Structures of active conformations of Giα1 and the mechanism of GTP hydrolysis. *Science.* 265:1405–1412.

Cooke, R. 1986. The mechanism of muscle contraction. *CRC Crit. Rev. Biochem.* 21:53–118.

Cremo, C. R. et al. 1990. *Biochemistry.* 29:3309–3319.

Crowder, M. C., and R. Cooke. 1987. The orientation of spin-labeled nucleotides bound to myosin in glycerinated muscle fibers. *Biophys. J.* 51: 323–333.

Franks-Skiba, K., and R. Cooke. 1995. The conformation of the active site of myosin probed using mant-nucleotides. *Biophys. J.* 68:142s–149s.

Franks-Skiba, K. et al. 1994. Quenching of fluorescent nucleotides bound to myosin: a probe of the active-site conformation. *Biochemistry.* 33: 12720–12728.

Gilson, M. K. et al. 1994. Open "back door" in a molecular dynamics simulation of acetylcholinesterase. *Science.* 263:1276–1278.

Henry, G. D. et al. 1993. Observation of multiple myosin subfragment 1-ADP-fluoroberyllate complexes by ^{19}F NMR spectroscopy. *Biochemistry.* 32:10451–10456.

Itakura, S. et al. 1993. Force-generating domain of myosin motor. *Biochem. Biophys. Res. Commun.* 196:1504–1510.

Jones, T. A. 1985. Interactive computer graphics: FRODO. *In* Methods in Enzymology. Academic Press, New York. 157–171.

Kraulis, P. J. 1991. MOLSCRIPT: a program to produce both detailed and schematic plots of protein structures. *J. Appl. Cryst.* 24:946–950.

Maruta, S. et al. 1993. Formation of stable myosin-ADP-alumium fluoride and myosin-ADP-beryllium fluoride complexes and their analysis using ^{19}F NMR. *J. Biol. Chem.* 268:7093–7100.

Merrit, E. A., and M. E. P. Murphy. 1994. Raster3D version 2.0: a program for photorealistic molecular graphics. *Acta Cryst.* D50:869–873.

Mornet, D. et al. 1979. The limited tryptic cleavage of chymotryptic S1: an approach to the characterization of the actin site in myosin heads. *Biochem. Biophys. Res. Commun.* 89:925–932.

Rayment, I., and H. M. Holden. 1994. The three-dimensional structure of a molecular motor. *Trends Biochem. Sci.* 19:129–134.

Rayment, I. et al. 1993a. Structure of the actin-myosin complex and its implications for muscle contraction. *Science.* 261:58–65.

Rayment, I. et al. 1993b. Three-dimensional structure of myosin subfragment-1: a molecular motor. *Science.* 261:50–58.

Rossmann, M. G. 1972. The Molecular Replacement Method. A Collection of Papers on the Use of Non-Crystallographic Symmetry. Gordon and Breach, New York.

Rypniewski, W. R. et al. 1993. Structural consequences of reductive methylation of lysine residues in hen egg white lysozyme: an x-ray analysis at 1.8 Å resolution. *Biochemistry.* 32:9851–9858.

Smith, T. J. 1993. MacInplot II—an updated program to display electron density and atomic models on the Macintosh personal computer. *J. Appl. Cryst.* 26:496–498.

Sondek, J. et al. 1994. GTPase mechanism of G proteins from the 1.7-Å crystal structure of transducin α-GDP-$AlF4^-$. *Nature.* 372:276–279.

Tronrud, D. E. et al. 1987. An efficient general-purpose least-squares refinement program for macromolecular structures. *Acta Cryst.* A43: 489–501.

Walker, J. E. et al. 1982. Distantly related sequences in the α- and β-subunits of ATP synthase, myosin, kinases, and other ATP-requiring enzymes and a common nucleotide binding fold. *EMBO J.* 1:945–951.

Warrick, H. M., and J. A. Spudich. 1987. Myosin structure and function in cell motility. *Annu. Rev. Cell Biol.* 3:379–421.

White, H. W., and I. Rayment. 1993. Kinetic characterization of reductively methylated myosin subfragment-1. *Biochemistry.* 32:9859–9865.

Yount, R. G. et al. 1992. Photochemical mapping of the active site of myosin. *Phil. Trans. R. Soc. Lond.* B336:55–61.

Yount, R. G. et al. 1995. Is myosin a "back door" enzyme? *Biophys. J.* 68:44s–49s.